Small Angle Neutron Scattering Study of Mixed AOT + Lecithin Reverse Micelles

Blake Simmons,[†] Vivek Agarwal,[‡] Gary McPherson,[§] Vijay John,*[,†] and Arijit Bose*[,‡]

Departments of Chemical Engineering and Chemistry, Tulane University, New Orleans, Louisiana 70118, and Department of Chemical Engineering, University of Rhode Island, Kingston, Rhode Island 02881

Received May 28, 2002. In Final Form: August 5, 2002

The structures formed in a four-component water-in-oil microemulsion consisting of deuterated water added to sodium bis(2-ethylhexyl) sulfosuccinate (AOT) and phosphatidycholine (lecithin) in 2,2,4-trimethylpentane (isooctane) have been probed by small-angle neutron scattering (SANS). The total surfactant concentration in each of the five samples studied is fixed at 0.01 M in isooctane. The water content is fixed at $W_t = 20$ (W_t = moles water/moles total surfactant). The molar ratios of lecithin to AOT are 0, 1:7, 1:3, 3:5, and 1:1 in the five samples, respectively. The experimental SANS data from all five samples are fit well by a model containing polydispersed spheres. The mean size of the spheres increases, whereas the polydispersity decreases as the lecithin content is increased. The different packing parameters for AOT and lecithin drive the observed changes in droplet size, whereas the reduction in polydispersity is a consequence of the increased rigidity of the interface as lecithin is added. An alternate morphology, consisting of prolate ellipsoids, also produces good fits to the SANS data. For this model, the ellipsoid volume increases, whereas the ratio of the major to minor axis goes toward unity as the lecithin content is increased. Radii of gyration obtained from fits in the Guinier/Zimm region match calculations from the droplet dimensions produced by fitting the complete scattering profiles. For lecithin/AOT molar ratios of 3/5 and 1, SANS measurements reveal that an attractive interaction develops between these droplets. The interdroplet interaction is described using a square well potential model. Fits to the SANS data give well depths of 0.022 and 0.126 kT, whereas the widths are 538 and 450 Å, respectively. The weak interaction over such long length scales is consistent with the formation of loosely bound clusters of microemulsion droplets at these lecithin concentrations.

1. Introduction

Surfactants have the ability to self-assemble into a wide variety of supramolecular structures such as micelles, bilayers, vesicles, liquid crystals, and emulsions.[1] Factors that determine the specific type of structure that is formed by a surfactant include the alkyl chain length,[2] the nature of the solvent, surfactant concentration,[3] temperature, salt concentration,[4] and the presence of a cosurfactant.[5]

The additional compositional degree of freedom available in mixed surfactant solutions allows a wider range of aggregate structures and morphologies than is possible in single surfactant systems. For example, aqueous mixtures of cationic and anionic surfactants form a rich variety of composition-dependent microstructures in solution including spherical micelles, wormlike mixed micelles, vesicles, and lamellar phases.[6] The expanded range of micellar geometries and functionalities available in mixed surfactant systems not only makes them useful for applications but also provides opportunities for fundamental studies of self-assembly. Typical length scales for these micelles are of the order of several nanometers. Thus, neutron scattering, where the probe wavelength is several angstroms, is a useful way to probe micellar structures.[6−8] Additional advantages include the ability to selectively deuterate desired components in a mixture, thus allowing specific domains to be observed, and the insensitivity to dust. In the experiments reported here, the "aqueous" phase is deuterium oxide (D_2O).

Our interest lies in the micelles formed by mixing the anionic surfactant AOT and the zwitterionic phospholipid lecithin with water and isooctane. We have previously reported on the rigid mesophase formed when water is added to a solution containing 0.8 M AOT and 0.4 M lecithin in isooctane for W_0 (molar ratio of water to AOT) values greater than 60.[9] The microstructure of this "gel" has been characterized extensively via small-angle neutron scattering (SANS).[10] As either the water content or temperature is varied, the microstructure undergoes a transition from columnar hexagonal to lamellar. This change in curvature is only present in the mixed surfactant system at these overall concentrations. It was hypothesized that the different surfactant packing parameters, P ($P = v/al$, where v is the volume occupied by the tails, a the effective area/headgroup, and l the maximum

* To whom correspondence should be addressed. Arijit Bose: Phone: 401-874-2804. E-mail: bosea@egr.uri.edu. Vijay John: Phone: 504-865-5883. E-mail: vijay.john@tulane.edu.

[†] Department of Chemical Engineering, Tulane University.

[‡] University of Rhode Island.

[§] Department of Chemistry, Tulane University.

(1) Imae, T. *Colloids Surf. A* **1996**, *109*, 291.

(2) Berlepsch, H. v.; Bottcher, C.; Ouart, A.; Regenbrecht, M.; Akari, S.; Keiderling, U.; Schnablegger, H.; Dahne, S.; Kirstein, S. *Langmiur* **2000**, *16*, 5908.

(3) Koehler, R. D.; Raghavan, S.; Kaler, E. W. *J. Phys. Chem. B* **2000**, *104*, 11025.

(4) Kumar, S.; Aswal, V. K.; Goyal, P. S.; Din, K. *J. Chem. Soc.* **1998**, *94*, 761.

(5) Freeman, K. S.; Tan, N. C.; Trevino, S. F.; Kline, S.; McGown, L. B.; Kiserow, D. J. *Langmuir* **2001**, *17*, 3912.

(6) Bergstrom, M.; Pedersen, J. S. *Langmuir* **1998**, *14*, 3754.

(7) Bumajdad, A.; Eastoe, J.; Heenan, R. K.; Lu, J. R.; Steytler, D. C.; Egelhaaf, S. *J. Chem. Soc.* **1998**, *94*, 2143.

(8) Bergstrom, M.; Pedersen, J. S. *J. Phys. Chem. B* **2000**, *104*, 4155.

(9) Li, S.; Irwin, G.; Simmons, B.; John, V.; McPherson, G.; Bose, A. *Colloids Surfaces A* **2000**, *174*, 275.

(10) Simmons, B.; Irvin, G. C.; Li, S.; John, V. T.; McPherson, G. L.; Balsara, N.; Agarwal, V.; Bose, A. *Langmuir* **2002,** *18*, 624.

10.1021/la026005m CCC: $22.00
Published on Web 10/03/2002

effective tail length), displayed by AOT ($P = 1.1$) and lecithin ($P = 0.6$) prompt a deformation of the spherical AOT reverse micelles as lecithin is added.

Cadmium sulfide nanoparticles formed by precipitation in the AOT/lecithin/isooctane/aqueous solution microemulsion change shape from spherical to acicular as the lecithin to AOT ratio in the microemulsion is increased from 0:1 to 1:1.[11] This dramatic change in nanoparticle morphology is potentially a templating effect, produced by changes in droplet shape when lecithin is added to the system.

Hence, in this paper, we look at mixtures of these surfactants formed at compositions just above the critical micelle concentration to uncover how lecithin perturbs the configuration of the reverse micelles. The surfactant concentration is deliberately kept low to minimize intermicellar interactions, allowing us to focus on the shape of individual micelles through the form factor component of the scattering profile. By probing the effects of binary surfactants on the resultant shape of the reverse micelles, a better understanding of self-assembly and microstructure may be obtained. From an applied perspective, these experiments may also help elucidate templating effects on nanoparticle synthesis, especially in situations where nonspherical nanoparticle morphologies are obtained.[11]

2. Materials and Methods

2.1. Chemicals. Lecithin (95% pure, extracted from soybeans) was obtained from Avanti Polar Lipids, Inc. Bis(2-ethylhexyl) sodium sulfosuccinate (AOT) and 2,2,4-trimethylpentane (isooctane, 99% purity) were purchased from Sigma-Aldrich. Deuterium oxide (99.9%) was purchased from Cambridge Isotopes Laboratory. All chemicals were used without further treatment or purification.

2.2. Samples. Five solutions were prepared. Each had an overall surfactant concentration of 0.01 M in isooctane, but had different molar proportions of lecithin and AOT. The solution compositions were (1) 0.01 M AOT with no lecithin, (2) 0.0875 M AOT/0.00125 M lecithin, (3) 0.0075 M AOT/0.0025 M lecithin, (4) 0.00625 M AOT/0.00375 M lecithin, and (5) 0.005 M AOT/0.005 M lecithin. Thus, the molar ratios of lecithin to AOT were 0:1, 1:7, 1:3, 3:5, and 1:1 in samples 1−5, respectively. Reverse micellar solutions were obtained by adding the exact amount of D_2O necessary to bring the $W_t = 20$ (W_t = moles D_2O/moles total surfactant). Because the total molar concentration of surfactant in isooctane does not vary, a fixed W_t ensures that the fraction of water in each of the samples is also identical. Observed changes in scattering profiles can then be assigned only to variations in size and morphology of the deuterated water droplets and interactions between them.

2.3. Experimental Details. SANS measurements were carried out on the 30 m NG3 beamline at the NIST Center for Neutron Research (Gaithersburg, MD). The instrument utilizes a mechanical velocity selector as a monochromator, a circular pinhole collimator, and a two-dimensional position sensitive detector (65 × 65 cm^2). The SANS intensity, I, was recorded as a function of the magnitude of the scattering vector q ($=4\pi \sin(\theta/2)/\lambda$, where θ is the scattering angle and λ is the neutron wavelength, equal to 6 Å). The detector angle was set at 2°, and the sample-to-detector distance was set to 2 m and 13 m to cover the widest possible range of q (0.004−0.6 $Å^{-1}$). Samples were contained in closed stainless steel cells with quartz windows that provided a path length of 2 mm. The sample temperature was maintained at 25 °C. The raw data was corrected for the scattering from an empty quartz cell, the detector sensitivity and background, the transmission of each sample, and placed on an absolute scale using software provided by NCNR. The primary component in our microemulsion system is isooctane. The spin contribution from hydrogen atoms and compositional contributions arising from differences in hydrogen and carbon cross-sections in isooctane are the major contributors to incoherent scatter. Therefore, this number[12] was subtracted from all our absolute intensity data prior to being reported and analyzed.

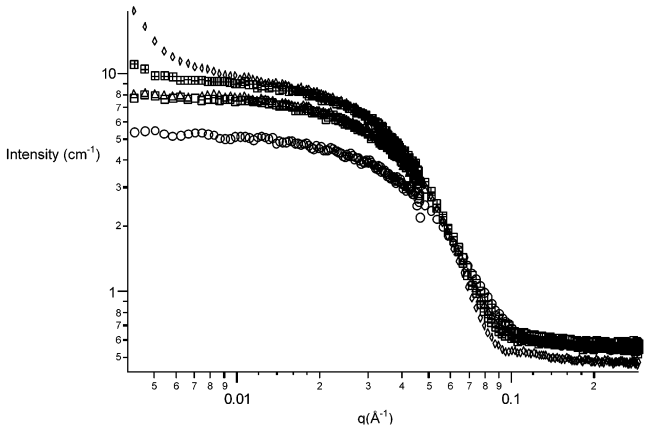

Figure 1. log−log plot of the intensity, I, versus magnitude of the scattering vector q. (○) 0.01 M AOT, sample 1; (□) 0.00125 M lecithin, 0.00875 M AOT, sample 2; (△) 0.0025 M lecithin, 0.0075 M AOT, sample 3; (⊞) 0.00375 M lecithin, 0.00625 M AOT, sample 4; (◇) 0.005 M Lecithin, 0.005 M AOT, sample 5. Samples 1−3 show a classical scattering profile, a low q asymptote (the Guinier/Zimm region), followed by a drop (fractal region), and then a decay at large q. Samples 4 and 5 shows an upturn in the intensity at low q, indicative of interactions between the scattering objects.

Table 1. Sample Compositions

sample	W_t = [D_2O]/[SURF]	total surfactant conc (M)	[lecithin]/[AOT]
1	20	0.01	0
2	20	0.01	1/7
3	20	0.01	1/3
4	20	0.01	3/5
5	20	0.01	1

3. Results and Discussion

A summary of all of the compositions of the samples used in this study is presented in Table 1. The corrected intensity data, $I(q)$, placed on an absolute scale, with incoherent scatter subtracted, is presented in Figure 1. They show the classical scattering profiles expected from micellar systems, a low q asymptote (the Guinier/Zimm region), followed by a (fractal) region, the Porod scatter from the interfaces, and then a decay at large q Note that as the lecithin content is increased, the slope of the curves in the Guinier/Zimm region changes systematically. Additionally, the slope in the "fractal" region (0.05 $Å^{-1} < q < 0.085$ $Å^{-1}$) changes systematically from −1.9 for sample 1 to −3 for sample 5, giving a first indication of the morphology of the scattering objects. Interestingly, as the lecithin content is increased, there is a noticeable upturn in the scattering profile at very low q, as shown in samples 4 and 5. We have used static and dynamic light scattering[13]

(11) Simmons, B.; Li, S.; John, V.; McPherson, G.; Bose, A. *Nano Lett.* **2002**, *2*, 263.

(12) Arleth, L.; Pedersen, J. S. *J. Appl. Cryst.* **2000**, *33*, 650.

(13) Agarwal, V. M.S. Thesis, University of Rhode Island, Kingston, RI, 2002.

Table 2. Radii of Gyration from Fits to Guinier/Zimm Region

sample	R_g (Å)	sample	R_g (Å)	sample	R_g (Å)
1	31.3 ± 0.2	3	36.1 ± 0.2	5	38.7 ± 0.2
2	35.6 ± 0.2	4	37.3 ± 0.1		

to further examine these samples; those results will be reported separately.

The scattering intensity obtained from an assembly of particles is given by[14]

$$I(q) = NK_iP(q)S(q) = I(0)P(q)S(q) \quad (1)$$

where N is the number of scattering centers, K_i is the contrast factor resulting from radiation of type i, $P(q)$ is the intraparticle form factor describing scattering for a single particle, and $S(q)$ is the structure factor accounting for interparticle interactions. In dilute systems, the intraparticle function $P(q)$ dominates the scattered intensity and $S(q)$ goes to unity, leading to

$$I(q) = NK_iP(q) = I(0)P(q) \quad (2)$$

At low q, the scattering intensity from a dilute system of noninteracting particles is independent of morphology, and is approximated by

$$\lim q \to 0, \frac{I(q)}{I(0)} = P(q) \sim \exp\left(\frac{-q^2R_g^2}{3}\right) \quad (3)$$

Here, R_g is the radius of gyration of the scattering objects. For spheres of radius R, the radius of gyration, R_g, is obtained from

$$R_g^2 = \frac{3}{5}R^2 \quad (4)$$

Equation 4 needs to be modified if the spheres are polydispersed. For a size distribution of spheres with a mean particle radius $\bar{R}$ and a standard deviation σ, the scattering intensity as $q \to 0$ is given

$$\lim q \to 0 \frac{I(q)}{I(0)} = \exp\left(\frac{-q^2\langle R^2\rangle}{5}\right) \quad (5)$$

leading to the following expression for the radius of gyration

$$R_g^2 = \frac{3\langle R^2\rangle}{5} \quad (6)$$

Here

$$\langle R^2\rangle = \bar{R}^2 + \sigma^2 \quad (7)$$

Plots of $\ln(I(q))$ versus q^2 in the Guinier/Zimm region have been used to obtain radii of gyration for the scattering objects in samples 1, 2, and 3. Samples 4 and 5 display upturns in intensity at low q. However, the length scale corresponding to the upturn is at least an order of magnitude larger than the droplet sizes (as shown later), validating a Guinier fit for these samples in the appropriate region. All of the radii of gyration produced this way are shown in Table 2. As lecithin is added to the system, there is a systematic increase in the radius of gyration of the water pools, from $R_g = 31.3$ Å for sample 1 to $R_g = 38.7$ Å for sample 5. Because the total water content in each of the samples is identical, this increase in R_g signifies an increase in the size and a decrease in number concentration of the droplets as lecithin is added.

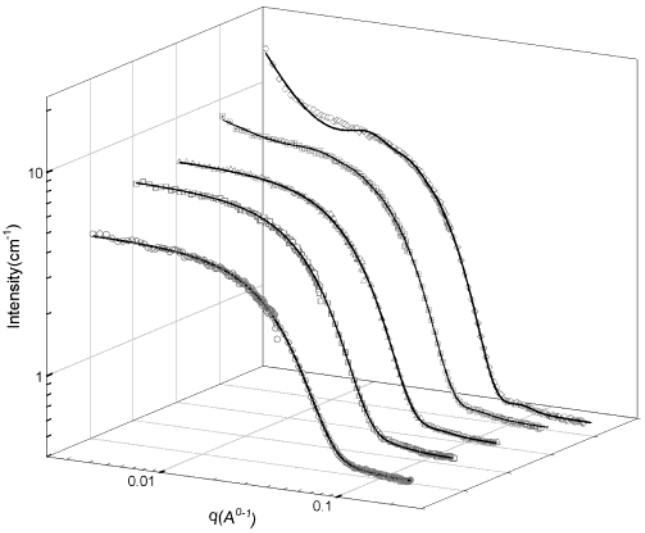

Figure 2. Plots showing the best fits to the SANS intensity data using the form factor for polydispersed spheres. A square well potential is used to describe the interactions in samples 4 and 5, to account for the upturn in the intensity at low values of q. (1) Sample 1. Mean radius = 30.5 Å, polydispersity = 0.26. (2) Sample 2. Mean radius = 36 Å, polydispersity = 0.23. (3) Sample 3. Mean radius = 39.2 Å, polydispersity = 0.19. (4) Sample 4. Mean radius = 42.5 Å, polydispersity = 0.17, well depth = 0.022 kT and well width = 588 Å. (5) Sample 5. Mean radius = 45 Å, polydispersity = 0.14, well depth = 0.126 kT and well width = 450 Å.

Slopes in the fractal region, identified to be between the Guinier/Zimm and Porod regions (0.05 Å$^{-1} < q < 0.085$ Å^{-1}) of plots of $\log(I)$ versus $\log(q)$ vary between -1.9 and -3. Thus, the microemulsion droplets are likely to be polydispersed spheres or ellipsoids with aspect ratios that are close to 1. To provide further information on the morphology of the water droplets, cross-section Guinier plots[15] of $\ln [Iq^x]$ versus q^2 were produced for all of the samples. The value of the exponent x that makes this plot linear in the fractal region is another indicator of the morphology of the scattering objects. For all our samples, we get the exponent $x = 0$, corresponding to scattering from spheres, and eliminating the possibility that the scattering is from long rods ($x = 1$) or lamellar phases ($x = 2$).

Each of the I(q) data sets were fitted using expressions for the form factors for polydispersed hard spheres[19] using the software IGOR PRO, and shown in Figure 2. The radius, polydispersity, volume fraction, and background intensity were the fitting parameters for the data in samples 1−3. The upturn in intensity at low q for samples 4 and 5 (Figure 1) is a signature of attractive interactions between the aqueous droplets. These interactions can give rise to formation of clusters, with a characteristic length $L \sim 2\pi/q_u$ where q_u is the value of q where the upturn begins. The length scale L is of the order of 500 Å, much larger than the surfactant tail lengths. This dimension is

(14) Guinier, A.; Fournet, G. *Small Angle Scattering of X-rays*; Wiley-Interscience: NewYork, 1955.
(15) Glatter, O.; Strey, R.; Schubert, K.-V.; Kaler, E. W. *Ber. Bunsen-Ges. Phys. Chem.* **1996**, *100*, 323.
(16) Kaler, E. W.; Billman, J. F.; Fulton, J. L.; Smith, R. D. *J. Phys. Chem.* **1991**, *95*, 461.
(17) Lee, C. T., Jr.; Johnston, K. P.; Dai, H. J.; Cochran, H. D.; Melnichenko, Y. B.; Wignall, G. D. *J. Phys. Chem. B* **2001**, *105*, 3545.
(18) Sharma, R. V.; Sharma, K. C. *Physica A* **1977**, *89*, 213.
(19) Griffith, W. L.; Triolo, R.; Compere, A. L. *Phys. Rev. A* **1987**, *35*, 2200.

Table 3. Droplet Dimensions and Fitted Parameters for Polydispersed Spheres

sample	radius (Å)	polydispersity	well depth (ϵ/kT)	well width (Å)	vol fract
1	30.5 ± 0.1	0.26	NA	NA	0.00429
2	36.0 ± 0.1	0.23	NA	NA	0.00453
3	39.2 ± 0.1	0.19	NA	NA	0.00434
4	42.5 ± 0.2	0.17	0.022	538 ± 13	0.00453
5	45.0 ± 0.6	0.14	0.126	450 ± 6	0.00438

an order of magnitude higher than that associated with the intermicellar attractive interactions in the AOT/water/near critical propane[16] and in the water-in-carbon dioxide microemulsions near the critical point.[17] The interaction energy $U(r)$ between the droplets is modeled using a square well potential of the form

$$U(r) = \infty, \quad r < 2\bar{R}$$
$$U(r) = -\epsilon, \quad 2\bar{R} \le r < 2\bar{R}\lambda$$
$$U(r) = 0, \quad r \ge 2\bar{R}\lambda \qquad (8)$$

Here r is the center-to-center distance between the droplets, $\bar{R}$ is the mean radius, ϵ is the depth and $2\bar{R}$ $(\lambda - 1)$ is the width of the well. In this model, the well width provides an estimate of the largest distance over which interdroplet interactions are significant, whereas the well depth is a measure of the strength of the interaction. An analytical expression for the structure factor corresponding to this potential is available[18] and is used in eq 1. For samples 4 and 5, the region $q > 0.018$ Å^{-1}, where the effects of droplet interactions are not significant, was fit using the radius, polydispersity, volume fraction and background intensity as four parameters. Using these values, the full range of the intensity data were then fitted with the depth and width of the square well as two new parameters.

The best-fit values of the width and depth of the square well potential model used for samples 4 and 5 are 538 Å and 0.022 kT for sample 4 and 450 Å and 0.126 kT for sample 5. These numbers imply extremely weak but rather long-range interactions between the droplets. Our interpretation is that the upturn reflects the formation of loosely bound clusters of droplets. The only potential impurities in our solutions are lipids of somewhat different molecular weight than lecithin (95% pure lecithin is used in these experiments). These impurities are not likely to produce aggregates of length scale ~50 nm. Thus, we believe that impurities are an unlikely cause for the increase in scattering intensity observed at low values of q.

The volume fractions obtained from the fits (Table 3) match well with the experimental value of 0.004. The mean sizes as well as the polydispersities (defined as the standard deviation σ divided by the mean radius $\bar{R}$) are shown in Table 3. As the lecithin content is increased, the mean size goes up, whereas the polydispersity decreases. For water-in-oil microemulsions, the droplet radius (assuming a Schultz size distribution[19]) as a function of water content is described by[20]

$$\bar{R}[1 + 2(\sigma/\bar{R})^2] \approx (3v/a)W_t \qquad (9)$$

where v is the molecular volume of water and a the average area/headgroup occupied by the surfactants at the interface. Table 4 shows the values of a calculated for our data using eq 9. a decreases systematically from 55.2 Å^2 for sample 1 to 39.2 Å^2 for sample 5, indicating a more dense surfactant film and greater rigidity at the interface as the lecithin content is increased. The observed decrease in polydispersity is also a consequence of this increased rigidity at the isooctane/water interface.

Table 4. Droplet Dimensions for Prolate Ellipsoids

sample	principal radius a (Å) (rotation axis)	principal radius b (Å)	a/b
1	63.0 ± 1.0	31.2 ± 0.6	2.0
2	67.0 ± 0.9	36.8 ± 0.5	1.8
3	65.7 ± 1.0	38.1 ± 0.5	1.7
4	62.9 ± 1.3	41.5 ± 0.6	1.5
5	63.2 ± 1.1	42.8 ± 0.5	1.5

The twin tailed anionic surfactant, AOT, typically forms spherical water-in-oil microemulsions.[21] AOT has a surfactant packing parameter, P, of 1.1 and tends to have a spontaneous curvature that is concave toward water.[22,23] Once above the critical micelle concentration, AOT spontaneously forms spherical reverse micelles. The zwitterionic surfactant phosphatidylcholine (lecithin) has a significantly larger headgroup and a smaller packing parameter of 0.6.[24] Thus, lecithin would form structures of lower curvature than AOT. Indeed, in nonpolar solvents, lecithin forms wormlike cylindrical reverse micelles that can incorporate water up to a water/lecithin molar ratio of 20.[25] When both surfactants are present, the droplets grow as lecithin is added, reflecting this geometric packing effect.

If the surfactant composition on the interface is nonuniform, with each dominating in regions of preferred curvature, then the spherical AOT reverse micelles can be deformed into prolate ellipsoids as lecithin is added to the system. In addition, the observed intensity data in the fractal region could also be obtained if the water droplets had ellipsoid shapes. Therefore, the SANS data was fitted using prolate ellipsoids[26] as the morphology of the droplets, and shown in Figure 3 (for samples 4 and 5, the fits are carried out in the region $q > 0.018$ Å^{-1} to avoid droplet interaction effects). The lengths of the major and minor axes resulting from these fits are reported in Table 5. Note that the fits to the prolate ellipsoid morphology are good. The ratio of the major to minor axis changes from 2 for sample 1 to 1.5 for sample 5. The approach of this ratio toward 1 as the lecithin content is increased is consistent with the increased rigidity of the interface. Because form factors for polydispersed spheres and prolate ellipsoids can be quite similar over the q range examined here, it is not surprising that this alternate model also fits the data. The picture that develops then is either polydispersed spheres with AOT/lecithin ratios varying between spheres, or ellipsoids where the AOT and lecithin compositions vary around an ellipsoidal interface. On the basis of this SANS data alone, it is not possible to discriminate between these droplet morphologies.

Equation 6 defines the mean radius of gyration for an assembly of polydispersed spheres. The radius of gyration

(20) Kotlarchyk, M.; Chen, S. H.; Huang, J. S.; Kim, M. W. *Phys. Rev. A* **1984**, *29*, 2054.

(21) Kotlarchyk, M.; Stephens, R. B.; Huang, J. S. *J. Phys. Chem.* **1988**, *92*, 1533.

(22) Israelachvili, J. N. *Intermolecular and Surface Forces*; Academic Press: New York, 1992.

(23) De, T. K.; Maitra, A. *Adv. Colloid Interface Sci.* **1995**, *59*, 193.

(24) Wabel, C. Ph.D. Dissertation, University of Erlangen, **1998**.

(25) Scartazzini, R.; Luisi, P. L. *J. Phys. Chem.* **1988**, *92*, 829. Capitani, D.; Segre, G. D.; Sparapani, R.; Giustini, M.; Scartazzini, R.; Luisi, P. L. *Langmuir* **1991**, *7*, 250. Schurtenberger, P.; Scartazzini, R.; Luisi, P. L. *Rheol. Acta* **1989**, *28*, 372.

(26) Luisi, P. L.; Scartazzini, R.; Haering, G.; Schurtenberger, P. *Colloid Polym. Sci.* **1990**, *268*, 356.

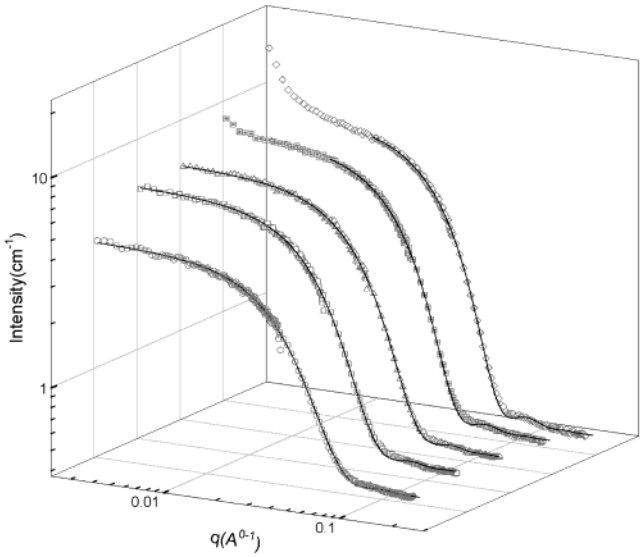

Figure 3. Plots showing the best fits to the SANS intensity data using the form factor for uniform prolate ellipsoids. To avoid structure factor effects in samples 4 and 5, only the region $q > 0.018$ Å^{-1} is used to fit the data. (1) Sample 1. Major axis $a = 63$ Å, minor axis $b = 31.2$ Å. (2) Sample 2. Major axis $a = 67$ Å, minor axis $b = 36.8$ Å. (3) Sample 3. Major axis $a = 65.7$ Å, minor axis $b = 38.1$ Å. (4) Sample 4. Major axis $a = 62.9$ Å and minor axis $b = 41.5$ Å. (5) Sample 5.Major axis $a = 63.2$ Å, minor axis $b = 42.8$ Å.

Table 5. Radii of Gyration

sample	radius of gyration from Guinier approximation (Å)	radius of gyration from droplet dimensions (Å) (polydisperse spheres)	radius of gyration from
1	31.3 ± 0.2	24.4	34.3
2	35.7 ± 0.2	28.6	38.8
3	36.2 ± 0.2	30.9	37.7
4	37.3 ± 0.1	33.4	38.7
5	38.7 ± 0.2	35.2	39.1

Table 6. Average Area/Headgroup

sample	average area/ headgroup a (Å^2)	sample	average area/ headgroup a (Å^2)
1	52.0	4	40.0
2	45.2	5	38.5
3	42.7		

of an ellipsoid with the principal axes a and b, where a is the radius of the rotation axis, is given by

$$R_g^2 = \left[\left(\frac{a}{5}\right)^2 + 2\left(\frac{b}{5}\right)^2\right] \quad (10)$$

Using the morphology and size data from the fits, the calculated radii of gyration are compared to the measured R_g from the Guinier analysis in Table 6. The maximum deviation for the spheres is 25%, whereas that for the ellipsoids is less than 10%.

We therefore summarize the interpretations to the scattering patterns in these dilute surfactant systems. With pure AOT as the surfactant, our observations are consistent with the literature that these are spherical droplets with a measure of polydispersity and with negligible droplet-droplet interactions at these low concentrations.[21] The partial substitution of lecithin for AOT, keeping overall concentration the same, leads to a larger size and greater interfacial rigidity. The increased interface rigidity causes a reduced polydispersity. Although we do not have direct evidence, there could also be a deformation of the droplets to a prolate ellipsoid morphology as lecithin is added. The tendency of AOT to occupy regions of higher curvature (about water) and the tendency of lecithin to form structures of lower curvature could lead to ellipsoids, with the high and low curvatures regions being rich in AOT and lecithin, respectively. The substitution of lecithin also leads to droplets with long-range attractive interactions over a distance of the order of 500 Å. This interaction is responsible for the formation of loosely bound clusters.

We note a very interesting observation here. In the synthesis of CdS nanoparticles in these mixed surfactant systems, we have seen a dramatic change in particle morphology, from quantum dots in the pure AOT system to highly acicular quantum rods in the 1:1 AOT:lecithin system.[11] These particle synthesis experiments were done at a surfactant concentration of 0.1 M, an order-of-magnitude higher than the surfactant concentrations (0.01 M) used in this study. Additionally, the structure of these CdS crystallites changes from the face-centered cubic in the quantum dot morphology to hexagonal in the quantum rod morphology. It is interesting to note that the length of these acicular particles is of the order of 50−100 nm, whereas the diameter is 4−5 nm. These length dimensions are much larger than the droplet dimension as probed by SANS at very low concentrations. Perhaps the length extension of these quantum rods is a function of the interaction and cluster formation of the droplets in the mixed surfactant system, rather than a direct templating effect.

4. Conclusions

Reverse micelles, formed by the addition of the anionic surfactant AOT and the zwitterionic surfactant lecithin to deuterated water/isooctane mixtures, have been analyzed at various AOT to lecithin molar ratios utilizing SANS. The key observations are an increase in droplet size, a fall in polydispersity, and the development of an attractive interaction between the droplets as the lecithin concentration is increased. The reduction in polydispersity is a consequence of increased rigidity of the surfactant film as lecithin is added. An alternate explanation for the observed scattering is that when both of the surfactants are present the surfactant composition is not uniform around the interface. Because AOT and lecithin have very different packing parameters, each favors regions of preferred curvature at the oil−water interface, leading to prolate ellipsoidal droplets. The weak attractive interaction over large length scales at high lecithin contents indicates the formation of loosely bound clusters. A comprehensive understanding of droplet shapes and interactions may have implications for the design of surfactant systems for templated materials synthesis.

Acknowledgment. We thank the NSF (9909912, 0092001) for support of this work and the NCNR at NIST for providing beam time for the experiments. We gratefully acknowledge the critical experimental support provided by B. Hammouda at NIST. We acknowledge vital contributions from N. Balsara and thank T. Lee, B. Hammouda, S. Kline, and A. C. Nunes for several important suggestions.

LA026005M